

Enriched Methane Production Through a Low Temperature Steam Reforming Reactor

Marcello De Falco

Abstract An innovative hybrid plant, composed by a solar section for heating up a molten salt stream through a Concentrating Solar Power (CSP) plant, a chemical section for the production of 1000 Nm³/h of Enriched Methane (EM) with a 20 %vol. content of hydrogen, and an electrical section for the electricity production by means of an Organic Rankine Cycle unit (conversion efficiency = 28 %) is presented and assessed. The core of the process is the low-temperature solar steam reformer, where a feedstock composed by methane and water steam is partially converted to hydrogen. The reactor is modeled in detail, the equations set is described and commented, together with the boundary conditions. Then, the reactors' behavior is simulated. By applying 15 reformers in parallel and imposing a Gas Hourly Space Velocity (GHSV) of 40,965 h⁻¹, it is possible to produce a stream of EM (20 %vol. H₂) equal to 1000 Nm³/h and 500 kW approximately of net electrical power output. The molten salt stream is heated up to 550 °C by the CSP plant, then it supplies the reforming process heat duty (reactor heat duty, feedstock preheating, and reactant steam generation) and, finally, it generates the electricity by exploiting its residual sensible heat. By the simulation of the reformers under industrial conditions, the feasibility of the proposed architecture is demonstrated and its potentialities are assessed.

Keywords Enriched methane production • CSP • Hybrid plant • Natural gas steam reforming

List of Symbols

C_i	i -component composition (mol m ⁻³)
c_p	Gas mixture specific heat (J kg ⁻¹ K ⁻¹)
$c_{p,MS}$	Molten salt specific heat (J kg ⁻¹ K ⁻¹)
CSP	Concentrating Solar Plant
D_{er}	Effective radial diffusivity (m ² s ⁻¹)

M. De Falco (✉)

University of Rome "Campus Bio-Medico", via Alvaro del
Portillo 21, 00128 Rome, Italy
e-mail: m.defalco@unicampus.it

d_p	Equivalent catalyst particle diameter (m)
EM	Enriched Methane
f	Friction factor
G	Superficial mass flow velocity ($\text{kg s}^{-1} \text{m}^{-2}$)
GHSV	Gas Hourly Space Velocity (h^{-1})
MDEA	Methyl diethanolamine
$n_{\text{reformers}}$	Number of reformers inside the shell
ORC	Organic Rankine Cycle
P	Reaction pressure (Pa)
PDE	Partial Differential Equation
PSA	Pressure Swing Adsorption
r	Radial coordinate (m)
r_i	Total reaction rate of the i -component ($\text{mol kg}_{\text{cat}}^{-1} \text{s}^{-1}$)
r_j	Reaction rate of reaction j ($\text{mol kg}_{\text{cat}}^{-1} \text{s}^{-1}$)
r_t	Catalytic tube radius (m)
T	Gas mixture temperature (K)
T_{MS}	Molten salt temperature (K)
U	Global heat exchange coefficient between the molten salt and reaction packed bed ($\text{J m}^{-2} \text{s}^{-1} \text{K}^{-1}$)
u_s	Gas velocity (m s^{-1})
w_{MS}	Molten salt mass flow rate (kg/s)
z	Axial coordinate (m)
ΔH_j	Enthalpy of reaction j (J mol^{-1})
ε	Void fraction of the catalytic bed
λ_{er}	Effective thermal conductivity ($\text{J m}^{-1} \text{h}^{-1} \text{K}^{-1}$)
μ_g	Gas mixture viscosity ($\text{kg m}^{-1} \text{K}^{-1}$)
ρ_B	Catalytic bed density (kg m^{-3})
ρ_g	Gas density (kg m^{-3})

1 Introduction

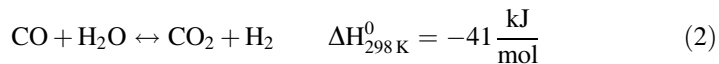
Many biological processes are proposed to produce enriched methane, as anaerobic fermentation of food wastes [1, 2], fermentation from waste lactose in cyclic-batch reactors [3], from xylose [4], or from wheat straw hydrolysate [5]. But, all the traditional chemical and electrochemical hydrogen production processes, as water electrolysis [6], hydrocarbons steam- and auto-thermal reforming [7, 8], and thermochemical cycles [9], can be used to produce enriched methane streams, simply adding methane at the end of the process or, if the methane is the feedstock, avoiding the last separation step between the hydrogen produced and the unreacted methane.

Among the traditional process for the massive industrial production of hydrogen, the natural gas steam reforming is the most used and technologically consolidated.

The process is composed of the Steam Reforming (SR) reaction (1)



which is strongly endothermic; and by the exothermic water gas shift (WGS) reaction (2)



The global reaction, described as follow:



is endothermic and needs a high-temperature thermal flux to be supported. Traditionally, the reactions are performed in catalytic tubular reactors placed inside a furnace, where the reactions (1–3) occur fast over Ni-based catalyst and when equilibrium conditions are quickly reached, so that high methane conversions (>90 %) are achieved only at high operating temperatures (850–1000 °C) [7].

But, if an enriched methane stream with a hydrogen content of 20–30 %vol. has to be produced instead of pure hydrogen, high methane conversions are not required and, consequently, the reactions can be performed at milder operating temperatures. From the thermodynamic analysis of the reactions (1–3) shown in Fig. 1, it can be noticed that a methane conversion of 10–20 %, enough to reach the process specification (20–30 %vol. of hydrogen in the outlet enriched methane mixture), is

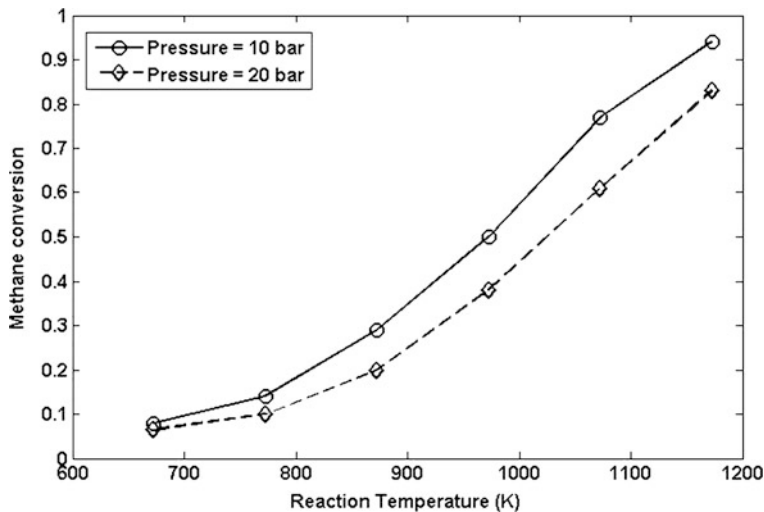


Fig. 1 Methane conversion at equilibrium conditions versus reaction temperature (H_2O to CH_4 ratio in the inlet feedstock equal to two)

achieved, at equilibrium conditions, at a reaction temperature within the range 500 °C (773 K) at 10 bar—550 °C (823 K) at 20 bar, leading to the possibility to avoid the use of a furnace for supplying the reactor heat duty.

The heat can be supplied coupling the methane steam reforming reaction with the Concentrating Solar Power (CSP) plant developed by ENEA and able to heat a thermal fluid (molten salt) up to 550 °C (823 K). Refer to chapter “[Methane/Hydrogen Mixtures from Concentrated Solar Energy: The METISOL Project](#)” for details about the CSP technology. By this configuration, the reaction operating temperature can reach 500–520 °C (773–793 K) and the equilibrium methane conversion is 15 % and more.

Such a solution leads to the following main benefits:

1. Since methane is the reaction feedstock, enriched methane mixture is directly produced in the reactor. Therefore, after the reaction, only separation steps to remove CO, CO₂, and steam water and to reach the final composition are required.
2. Natural gas steam reforming is a consolidated and widely applied process, so that the technology is well-known and a wide industrial experience is available.
3. The coupling between the enriched methane production process and the molten salt-based CSP technology is feasible since the thermal flow generated by the solar plant has the proper thermal level for the EM production through steam reforming.

In this chapter, after the description of the process configuration and its comparison with the traditional natural gas steam reforming plant, a mathematical model of the low-temperature solar steam reforming reactor for the enriched methane (EM) mixture production is presented and described. Then, some simulations imposing industrial conditions (1.000 Nm³/h of EM production) are reported and results are discussed, demonstrating the feasibility of the technological solution.

2 Solar Steam Reforming Process

As above mentioned, the natural gas steam reforming is a consolidated industrial process widely applied for the massive production of pure hydrogen. Figure 2 shows a layout of the complete process, which is composed by

- A pretreatment section, where the methane is compressed (C-1), the water stream is pumped (P-1), and then vaporized (E-1); the two streams are mixed and pre-heated (E-2) before entering into the reactor;
- A reaction section, composed by the catalytic tubular reactors (R-1) placed inside a furnace, where the required high operating temperatures are reached;
- A purification section, where unreacted steam is separated by condensation (E-3 + V-1), CO₂ by an ammine separation unit (MDEA, S-1), while produced hydrogen and un-reacted methane are separated by a Pressure Swing Adsorption (PSA) unit (S-2).

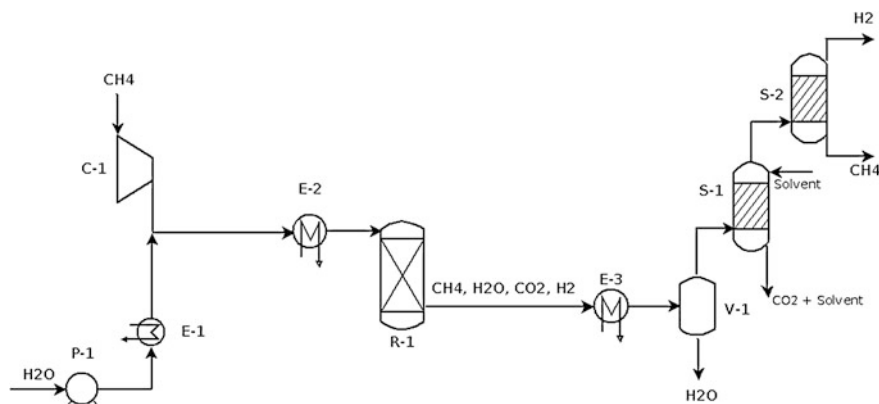


Fig. 2 Methane steam reforming traditional process layout

When the scope of the process is the production of EM instead of pure hydrogen, the last separation step (PSA) can be avoided and replaced by a methane stream addition, needed to modulate the hydrogen content in the final mixture. Moreover, the reactors are not placed in a furnace but they are tubes-and-shell shaped, with the hot molten salt stream fed through the shell. The molten salt supplies the heat for the reactor duty, for the preheating of the feedstock (E-2) and for the reactant steam generation (E-1).

Figure 3 reports a layout of the steam reforming process for the enriched methane production

- the feedstock is compressed (CH_4) and pumped (H_2O) up to the reaction pressure;
- the liquid water is vaporized by means of the boiler E-1;
- then, the reactant mixture is preheated by E-2 up to the reactor's operating temperature;

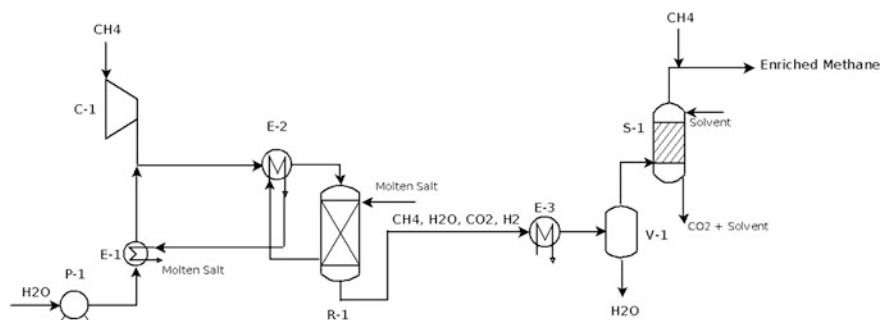


Fig. 3 Solar steam reforming for enriched methane production process layout

- the reactants are fed to the reactor R-1, where the low-temperature steam reforming reactions (1–3) are supported by exploiting the sensible heat of the hot molten salt stream, heated up by the CSP plant;
- the un-reacted water is separated by condensation;
- the CO_2 is separated in an MDEA unit (S-1);
- at the end, a methane stream is added to the final mixture to modulate the hydrogen content in the EM stream.

After supplying the heat needed for the enriched methane generation, the molten salt stream still has a high level of sensible heat, which can be exploited to produce medium pressure steam to be sent to a steam turbine for electricity production. By this configuration, the CSP-EM production plant is cogenerative, since it is able to produce both the hydrogen in the EM mixture and an electricity output exploiting solar energy.

The core of the process is the low-temperature steam reforming reactor, heated up by the molten salt stream and where the reactions occur at a temperature within the range 500–520 °C. In the next paragraph, a detailed mathematical model for the design and simulation of the reformer behavior is presented and discussed.

3 Solar Steam Reforming Reactor Modeling

The low-temperature steam reforming reactor is modeled by means of material, energy, and momentum balances. The reformer is assumed to be a tubes-and-shell unit, where the molten salt stream is fed through the shell and the reactants mixture through the tubes, as shown in Fig. 4.

The model is composed by a set of Partial Differential Equations (PDEs) able to simulate the axial and radial profiles (two-dimensional model) of components' concentration, temperature, and pressure inside the cylindrical reformers. The balances are imposed with the following assumptions:

- steady-state conditions;
- a single tube is representative of any other tube;

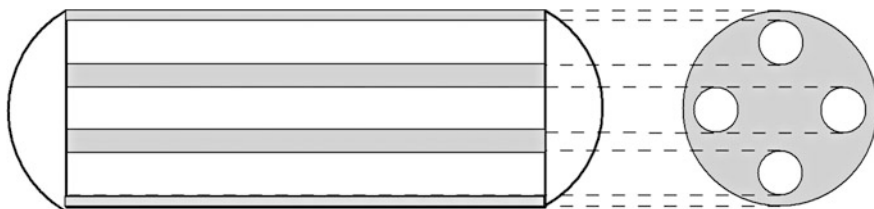


Fig. 4 Solar reformer tubes-and-shell shaped configuration

- pseudo-homogenous conditions, i.e., the packed bed reactor is described without considering the existence of two different phases (gas mixture and catalytic solid). The balances are imposed for one single pseudo-phase and the chemical–physical properties and transport coefficients are calculated by applying empirical expressions reported in the literature [10, 11];
- plug-flow is imposed for the gas velocity profiles, leading to a uniform pressure profile in the radial coordinate;
- axial mixing is neglected, and the only transport mechanism along the axial coordinate is the convective flux;
- pressure drop in the shell is neglected;
- one-dimensional energy balance in the shell is imposed.

A complete description of the model is reported in [12]. Here, the main equations composing the PDEs set to be solved, together with the boundary conditions, are listed

Material balances in the tubes

$$\frac{\varepsilon D_{\text{er}}}{u_s} \left(\frac{\partial^2 (u_s C_i)}{\partial r^2} + \frac{1}{r} \frac{\partial (u_s C_i)}{\partial r} \right) - \frac{d(u_s C_i)}{dz} = \rho_B r_i \quad (4)$$

where ε is the void fraction of the catalytic bed, D_{er} the effective radial diffusivity of the pseudo-homogeneous phase [10], u_s the gas velocity, C_i the i -component composition, r the radial coordinate, z the axial coordinate, ρ_B the catalytic bed density, and r_i the total reaction rate of the i -component, calculated according to the Xu-Froment mechanism [13].

Energy balance in the tubes

$$-\lambda_{\text{er}} \left(\frac{\partial^2 T}{\partial r^2} + \frac{1}{r} \frac{\partial T}{\partial r} \right) + u_s \rho_g c_p \frac{dT}{dz} = \sum_{j=1}^{n_r} (-\Delta H_j) \rho_B r_j \quad (5)$$

where λ_{er} is the effective thermal conductivity of the pseudo-homogeneous phase [10], T the gas mixture temperature, ρ_g the gas density, c_p the gas mixture specific heat, ΔH_j , and r_j the enthalpy and the reaction rate of reaction j ($=1, 2, 3$), respectively.

Energy balance in the shell

$$w_{\text{MS}} c_{p,\text{MS}} \frac{dT_{\text{MS}}}{dz} = \pm U \cdot n_{\text{reformers}} \cdot 2 \cdot \pi \cdot r_t \cdot (T_{\text{MS}} - T) \quad (6)$$

where w_{MS} is the mass flow rate of the molten salt stream, $c_{p,\text{MS}}$ its specific heat, T_{MS} the temperature of the molten salt, U the global heat exchanging coefficient between the tubes and the shell [14], $n_{\text{reformers}}$ the number of the tubes inside the

shell, and r_t the tubes radius. The sign \pm represents that the molten salt stream can be fed co-currently ($-$) or counter-currently ($+$).

Momentum balance in the tubes

$$\frac{dP}{dz} = - \frac{f \cdot G \cdot \mu_g}{\rho_g d_p^2} \cdot \frac{(1 - \varepsilon)^2}{\varepsilon^3} \quad (7)$$

where P is the reaction pressure, f the friction factor, G the superficial mass flow velocity, μ_g the gas mixture viscosity, d_p the equivalent catalyst particle diameter.

The boundary conditions to be imposed to solve the PDEs set (4)–(7) are

$$\begin{aligned} z = 0, \forall r : \\ u_s C_i &= (u_s C_i)_{\text{in}} \\ T &= T_{\text{in}} \\ P &= P_{\text{in}} \\ T_{\text{MS}} &= T_{\text{MS,in}} \quad \text{heat exchange co-current configuration} \end{aligned} \quad (8)$$

$$\begin{aligned} z = L, \forall r : \\ T_{\text{MS}} &= T_{\text{MS,in}} \quad \text{heat exchange counter-current configuration} \end{aligned} \quad (9)$$

$$\begin{aligned} r = r_t, \forall z : \\ \frac{\partial(u_s \cdot c_i)}{\partial r} &= 0 \\ \lambda_{\text{er}} \cdot \frac{\partial T_{\text{reac}}}{\partial r} &= U \cdot (T_{\text{MS}} - T|_{r_t}) \end{aligned} \quad (10)$$

$$\begin{aligned} r = 0, \forall z : \\ \frac{\partial(u_s \cdot c_i)}{\partial r} &= 0 \\ \frac{\partial T}{\partial r} &= 0 \end{aligned} \quad (11)$$

Solving the proposed PDEs set by applying the boundary conditions (8)–(11) it is possible to calculate the radial and axial profiles of the components' concentration and of the reaction temperature, the axial profile of the reaction pressure, and the axial profile of the molten salt temperature.

In the following, some simulations imposing industrial conditions (1.000 Nm³/h of EM production) are reported in order to assess the low-temperature steam reforming reactor behavior and the technology potentialities.

4 Industrial Reactor Simulation and Performance Analysis

A deep analysis of the effect of the main operating conditions as the reaction temperature and pressure, the reactants mixture residence time, the inlet feedstock composition, etc. is reported in [15]. Here, a preliminary design of the low-temperature solar reformer operating under industrial conditions is proposed by exploiting the mathematical model described in the previous paragraph.

It is assumed that after the reformer, a WGS reactor able to convert the 99 % of CO produced by reaction (1) in CO₂ and H₂ by supporting the reaction (2) is integrated. Moreover, the molten salt stream, after supplying the reaction heat duty, is fed to the reactant steam generator and then to an Organic Rankine Cycle (ORC) for the production of electricity with a conversion efficiency, calculated as the ratio between the electrical output and the residual sensible heat of the molten salt stream, equal to 28 %, so that the produced electrical power is

$$P_{el} = 0.28 \cdot w_{MS} c_{p,MS} (T_{out,MS} - 290^{\circ}\text{C}) \quad (12)$$

where $T_{out,MS}$ is the temperature of the molten salt stream after the EM production plant.

The fixed parameters for the reactor simulation are summarized in Table 1.

The process specific is the production of 1000 Nm³/h of EM with a content of 20 %vol. H₂. Such specificity is obtained by modulating the following operation and configuration parameters

- the Gas Hourly Space Velocity, i.e.,

$$\text{GHSV} = \frac{Q_{\text{feedstock}}}{V_{\text{reformers}}} \quad (\text{h}^{-1}) \quad (13)$$

where $Q_{\text{feedstock}}$ is the total volumetric inlet flow rate and $V_{\text{reformers}}$ is the total volume of the number of installed reformers ($n_{\text{reformers}}$);

- the number of reformers $n_{\text{reformers}}$ installed inside the shell of the tubes-and-shell shaped reactor (refer to Fig. 4).

Table 1 Process parameters fixed in the simulation

Inlet temperature T_{in} (°C)	500
Inlet pressure P_{in} (bar)	10
Steam to carbon ratio	3
Molten salt mass flow rate w_{MS} (kg/s), fed co-currently with the reactants flow	6
Molten salt inlet temperature $T_{MS,in}$ (°C)	550
Reactor length L (m)	2.05
Reactor external radius r_r (cm)	4.8

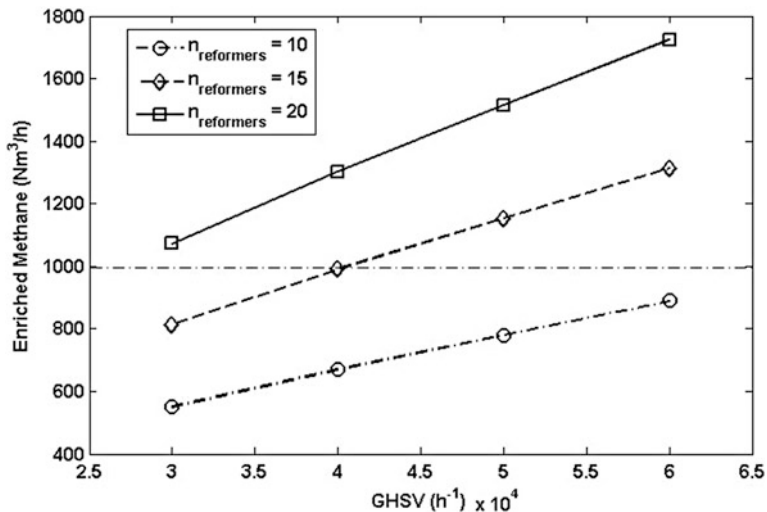


Fig. 5 Enriched methane production versus Gas Hourly Space Velocity at various number of reformers in parallel

Figure 5 shows the total enriched methane (20 %vol. of H_2) produced varying the GHSV and imposing $n_{\text{reformers}} = 10, 15$, and 20 in parallel.

Increasing the GHSV leads to an increase of EM production since, fixing the reformers volume, increasing GHSV means that higher methane and steam flow rates are fed to the reactors. Moreover, installing more reformers in parallel leads to an increase in EM production.

Fixing a number of reformer equal to 15 and a GHVS of $40,965 \text{ h}^{-1}$ ($359 \text{ Nm}^3/\text{h}$ of methane + $1077.7 \text{ Nm}^3/\text{h}$ of steam water), which is a realistic value for an industrial application, the following results are obtained:

- methane conversion = 14.02 %
- hydrogen outlet flow rate = $201.54 \text{ Nm}^3/\text{h}$
- hydrogen content in the EM mixture after the reactor and the separation steps = 39.5 %vol.
- final molten salt temperature = $483.6 \text{ }^\circ\text{C}$

As shown in the Fig. 3, after the reaction and H_2O and CO_2 separation, a methane flow is added to regulate the final H_2 composition in the EM mixture: therefore, $497.3 \text{ Nm}^3/\text{h}$ of methane is added and the final target of $1000 \text{ Nm}^3/\text{h}$ of EM with 20 %vol. of H_2 is achieved (as shown in Fig. 5).

Then, the residual molten salt stream sensible heat is used to generate an electrical power output equal to $499.8 \text{ kW}_{\text{el}}$.

Figure 6 shows the axial profile of the temperature inside the reactor in three different radial coordinates and the axial profile of the molten salt temperature. It is clear that the axial profiles present a “cold spot” in the first part of the reactor, where the endothermic reaction is strongly supported; then, the reaction kinetics is low,

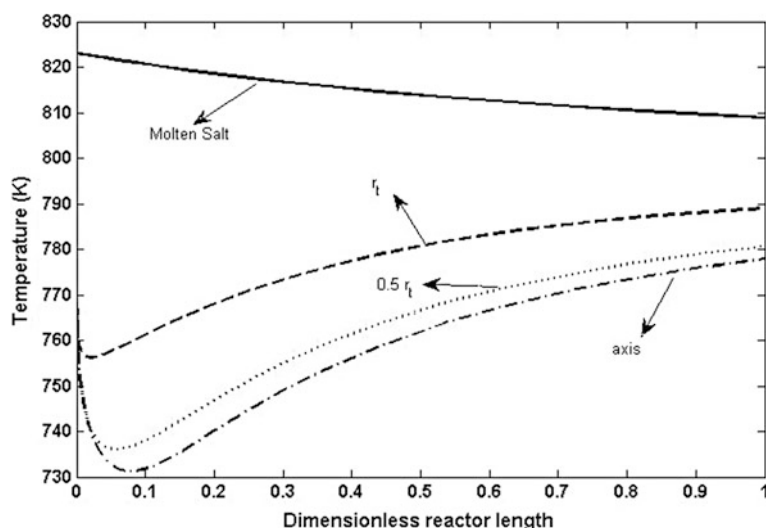


Fig. 6 Temperature profiles of the molten salt stream and inside the reactor

since the products composition increases and the temperature grows, thanks to the heat flow from the molten salt. In the radial direction, it has to be noticed that a high-temperature radial gradient is present (12 °C approximately from the reformer wall to the center).

Figure 7 illustrates the components' molar fraction inside the reactor (averaged on the radial coordinate). It is worth the assessment that a steep increase of

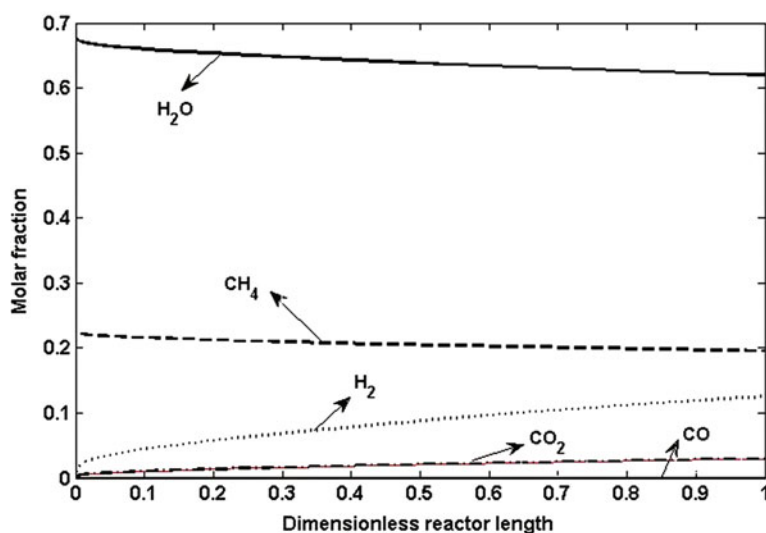


Fig. 7 Molar fraction of the components inside the reactor

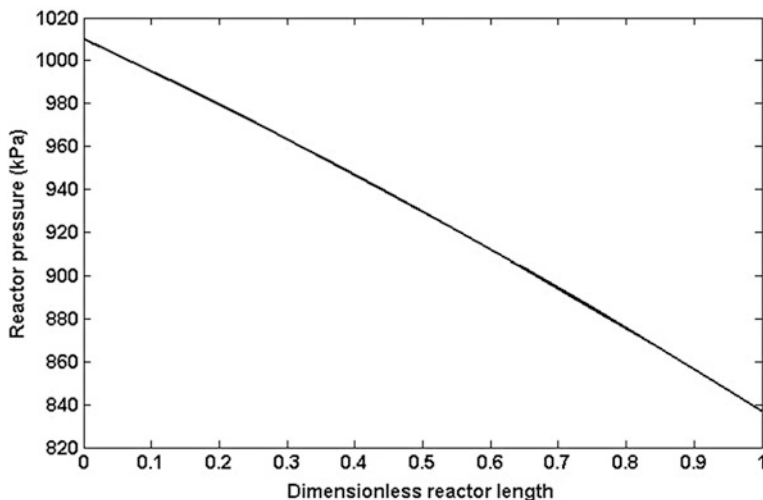


Fig. 8 Reaction pressure profile inside the reactor (1 bar = 100 kPa)

hydrogen content in the mixture occurs inside the reactor, while the CO_2 and mainly the CO molar fraction are always low: in the outlet stream, the molar fraction of CO_2 is 0.03, while the molar fraction of CO is 10^{-5} .

Finally, the pressure axial profile inside the reactor is shown in Fig. 8. A pressure drop equal to 2.4 bar approximately occurs inside the reactor, which is an admissible value for the application.

5 Conclusions

A low-temperature solar steam reformer, heated up by the molten salt stream of a CSP plant, has been modeled and simulated under industrial environments.

Imposing the conditions listed in Table 1, by applying 15 reformers and a GHSV of $40,965 \text{ h}^{-1}$, it is possible to produce a stream of EM equal to $1000 \text{ Nm}^3/\text{h}$ and 500 kW approximately of electrical power output, generated by exploiting the residual sensible heat of the molten salt stream.

The simulation has demonstrated the feasibility of the proposed hybrid architecture, composed by a solar section for heating up the molten salt, a chemical section for the EM production, and an electrical section for the electricity production.

The EM produced can be stored in traditional methane storage system or fed to the natural gas medium pressure distribution network [16] and used as a feedstock for the natural gas fuelled Internal Combustion Engines (ICE), with an improvement of the engine conversion efficiency and a reduction of carbon dioxide and pollutants emissions [17, 18].

The plant proposed is composed by consolidated technologies (molten salt CSP, natural gas steam reforming process, and ORC unit), leading to a high level of operational reliability.

References

1. Cavinato C, Bolzanella D, Fatone F, Cecchi F, Pavan P (2011) Optimization of two-phase thermophilic anaerobic digestion of biowaste for hydrogen and methane production through reject water recirculation. *Bioresour Technol* 102:8605–8611
2. Cavinato C, Giuliano A, Bolzonella D, Pavan P, Cecchi F (2012) Bio-hythane production from food waste by dark fermentation coupled with anaerobic digestion process: a long-term pilot scale experience. *Int J Hydrogen Energy* 37:11549–11555
3. Clark IC, Zhang RH, Upadhyaya SK (2012) The effect of low pressure and mixing on biological hydrogen production via anaerobic fermentation. *Int J Hydrogen Energy* 37:11504–11513
4. Kongjan P, Min B, Angelidaki I (2009) Biohydrogen production from xylose at extreme thermophilic temperatures (70 C) by mixed culture fermentation. *Water Res* 43:1414–1424
5. Pawar SS, van Niel EWJ (2013) Thermophilic biohydrogen production: how far are we? *Appl Microbiol Biotechnol* 97:7999–8009
6. Zeng K, Zhang D (2010) Recent progress in alkaline water electrolysis for hydrogen production and applications. *Prog Energy Combust Sci* 36:307–326
7. Rostrup-Nielsen JR (1984) Catal Steam Reform. *Catalysis* 5:1–117
8. Li Y, Wang Y, Zhang X, Mi Z (2008) Thermodynamic analysis of autothermal steam and CO₂ reforming of methane. *Int J Hydrogen Energy* 33:2507–2514
9. Steinfeld A (2005) Solar thermochemical production of hydrogen—a review. *Sol Energy* 78:603–615
10. Kulkarni B, Doraiswamy L (1980) Estimation of effective transport properties in packed bed reactors. *Catal Rev Sci Eng* 22:431–483
11. Dixon A, Cresswell D (1979) Theoretical prediction of effective heat transfer parameters in packed beds. *AIChE J* 25:663–675
12. De Falco M, Giaconia A, Marrelli L, Tarquini P, Grena R, Caputo G (2009) Enriched methane production using solar energy: an assessment of plant performance. *Int J Hydrogen Energy* 34:98–109
13. Xu J, Froment G (1989) Methane steam reforming, methanation and water-gas shift: I intrinsic kinetics. *AIChE J* 35:88–96
14. De Falco M (2011) Membrane reactor modeling. In: De Falco M, Marrelli L, Iaquaniello G (eds) *Membrane reactors for hydrogen production processes*. Springer, New York. ISBN:978-0-85729-150-9
15. De Falco M, Piemonte V (2011) Solar enriched methane production by steam reforming process: reactor design. *Int J Hydrogen Energy* 36:7759–7762
16. Haeseldonckx D, D’haeseleer W (2007) The use of natural-gas pipeline infrastructure for hydrogen transport in a changing market structure. *Int J Hydrogen Energy* 32:1381–1386
17. Orhan Akansu S, Dulger Z, Kaharaman N, Veziroglu TN (2004) Internal combustion engines fuelled by natural gas–hydrogen mixtures. *Int J Hydrogen Energy* 29:1527–1539
18. Ortenzi F, Chiesa M, Scarcelli R, Pede G (2008) Experimental tests of blends of hydrogen and natural gas in light-duty vehicles. *Int J Hydrogen Energy* 33:3225–3229

Enriched Methane

The First Step Towards the Hydrogen Economy

De Falco, M.; Basile, A. (Eds.)

2016, VIII, 257 p., Hardcover

ISBN: 978-3-319-22191-5